SML SOFT MACHINES LAB integrated soft materials for human-compatible machines and electronics

Carnegie Mellon University

Trajectory Optimization for Thermally-Actuated Soft Planar Robot Limbs

Anthony Wertz (me), Andrew P. Sabelhaus, Carmel Majidi

April 22, 2022

A. Wertz, A. P. Sabelhaus, and C. Majidi, "Trajectory optimization for thermally-actuated soft planar robot limbs," in *IEEE 5th International Conference on Soft Robotics (RoboSoft)*. 2022.

Project at a glance

- Sensorizing a compliant, thermally actuated robot limb
- Develop simplified system model
- Calibrate model parameters
- Trajectory optimization for open-loop control
- Validate in hardware
- Future directions

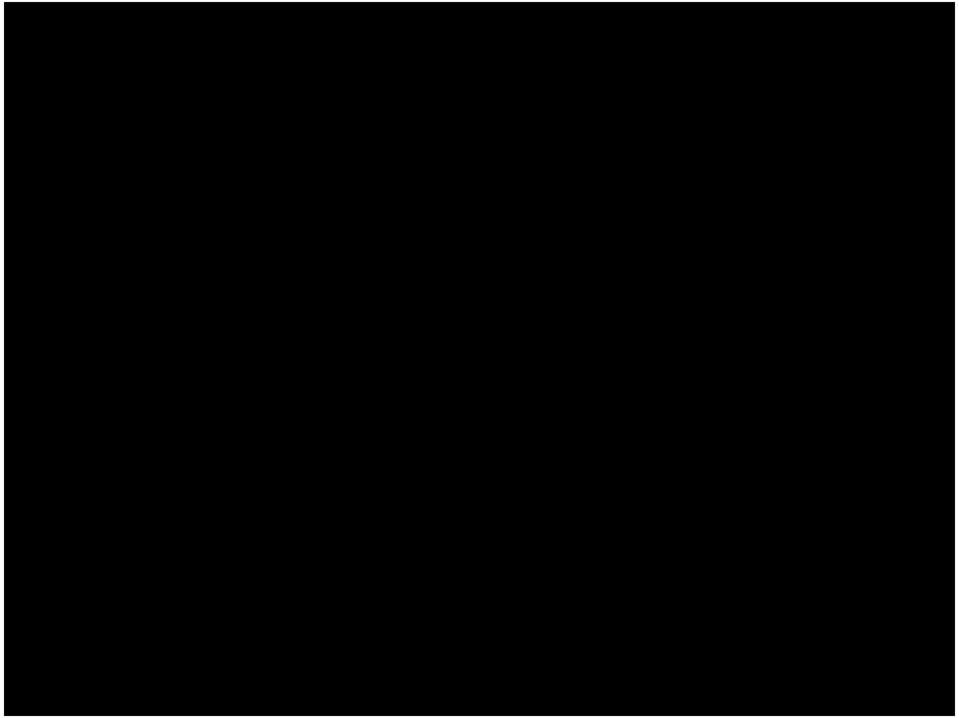

A. Wertz, A. P. Sabelhaus, and C. Majidi, "Trajectory optimization for thermally-actuated soft planar robot limbs," in *IEEE 5th International Conference on Soft Robotics (RoboSoft)*. 2022.

Overview

Background, Hardware, Experiment

Background

Background

Soft systems are hard to model

- Kinematics hard - “Infinite” DoF
- Dynamics hard - Continuum deformation and rate-dependent mechanics

Background

Soft systems are hard to model

- Kinematics hard - “Infinite” DoF
- Dynamics hard - Continuum deformation and rate-dependent mechanics

Thermal actuation of shape memory alloy (SMA) is hard to model

- Difficult/impossible to measure metallurgical state
- Difficult to deal with hysteresis

Background

Soft systems are hard to model

- Kinematics hard - “Infinite” DoF
- Dynamics hard - Continuum deformation and rate-dependent mechanics

Thermal actuation of shape memory alloy (SMA) is hard to model

- Difficult/impossible to measure metallurgical state
- Difficult to deal with hysteresis

Open-loop control not well-explored

- Since modeling is difficult, mostly just use some form of sensing and control
- Not as good for untethered applications or planning

Hardware configuration

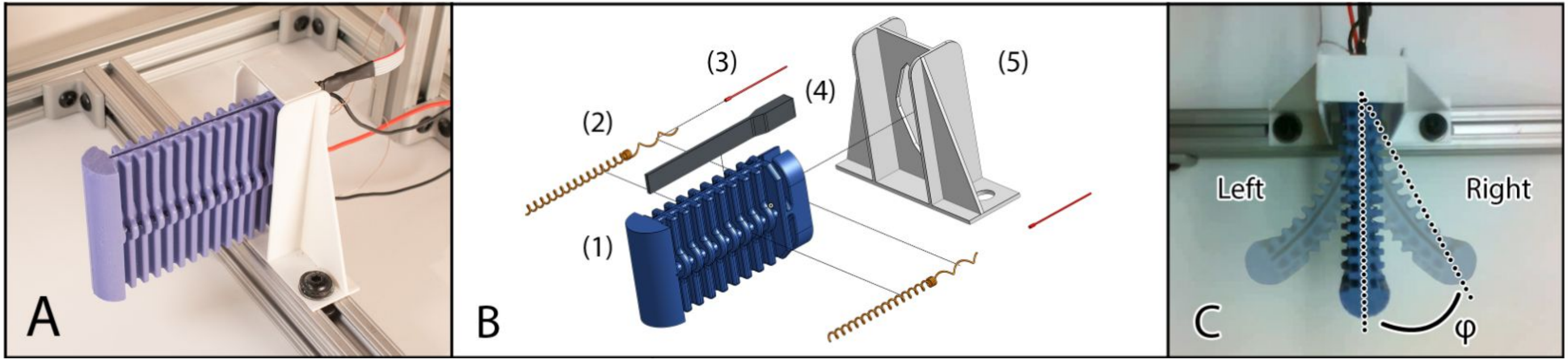

A. Cast silicone limb mounted to test fixture

B. Exploded view of limb (1), SMA actuators (2), thermocouples (3), bend sensor (4), and mounting bracket (5)

C. Top down view of actuation and bend angle

Data flow and experimental design

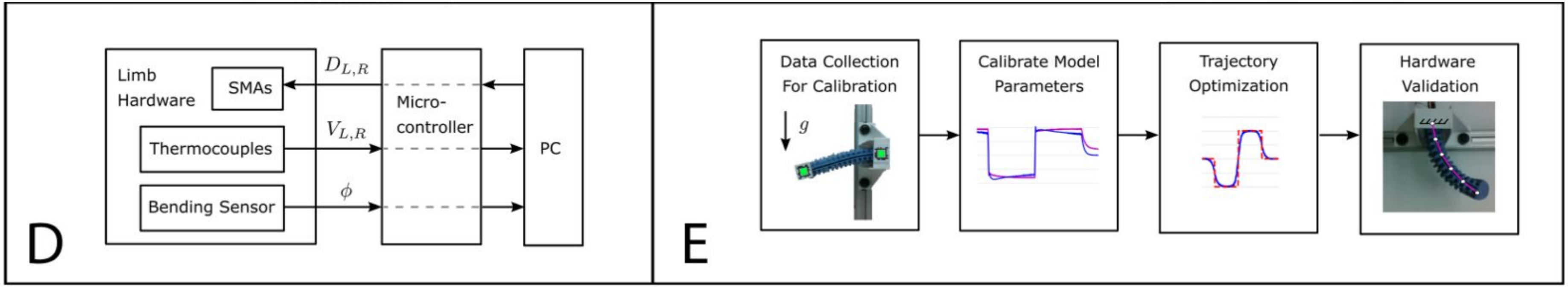

D. Data flow diagram

E. Experimental design

Dynamics Modeling

Continuum limb, Thermal actuator

Continuum limb manipulator model

- Used typical rigid link manipulator model
  - Alternatives exist, namely DER

$$\mathbf{M}(\boldsymbol{\theta})\ddot{\boldsymbol{\theta}} + \mathbf{C}(\boldsymbol{\theta}, \dot{\boldsymbol{\theta}})\dot{\boldsymbol{\theta}} + k\boldsymbol{\theta} + \sigma\dot{\boldsymbol{\theta}} = \mathbf{f}(\mathbf{T}).$$

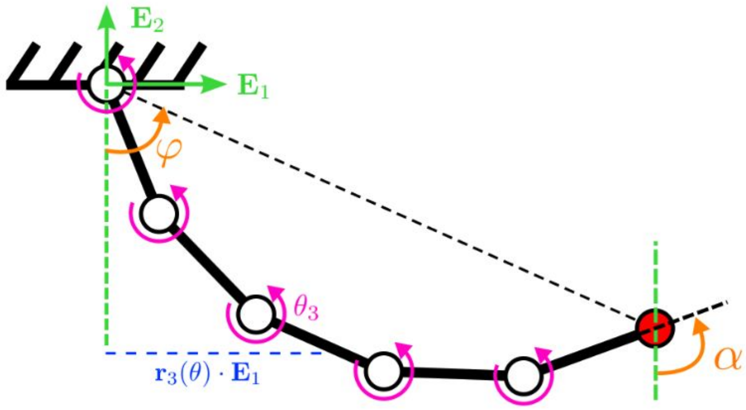

Continuum limb manipulator model

- Used typical rigid link manipulator model
  - Alternatives exist, namely DER
- Added:
  - Torsional spring at joints

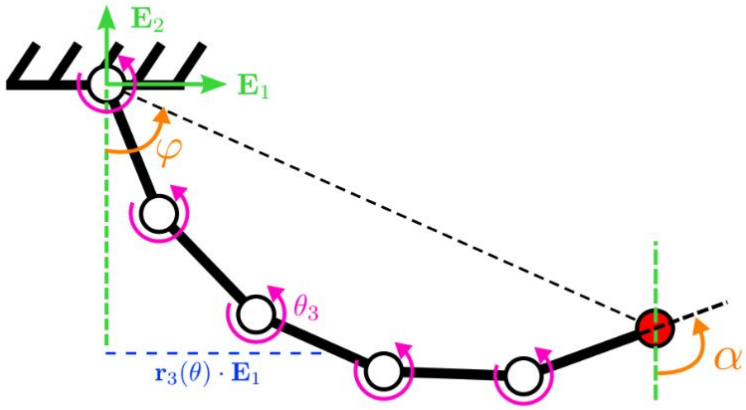

$$\mathbf{M}(\boldsymbol{\theta})\ddot{\boldsymbol{\theta}} + \mathbf{C}(\boldsymbol{\theta}, \dot{\boldsymbol{\theta}})\dot{\boldsymbol{\theta}} + \boxed{k\boldsymbol{\theta}} + \sigma\dot{\boldsymbol{\theta}} = \mathbf{f}(\mathbf{T}).$$

Continuum limb manipulator model

- Used typical rigid link manipulator model
  - Alternatives exist, namely DER
- Added:
  - Torsional spring at joints
  - Viscous damping

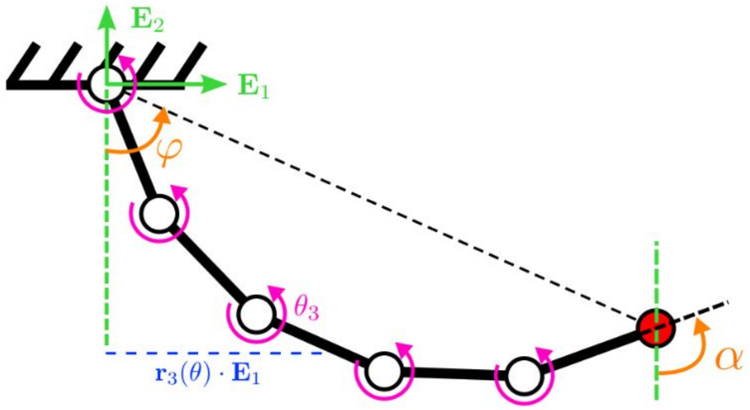

$$\mathbf{M}(\boldsymbol{\theta})\ddot{\boldsymbol{\theta}} + \mathbf{C}(\boldsymbol{\theta}, \dot{\boldsymbol{\theta}})\dot{\boldsymbol{\theta}} + \boxed{k\boldsymbol{\theta}} + \boxed{\sigma\dot{\boldsymbol{\theta}}} = \mathbf{f}(\mathbf{T}).$$

Continuum limb manipulator model

- Used typical rigid link manipulator model
  - Alternatives exist, namely DER
- Added:
  - Torsional spring at joints
  - Viscous damping
  - Actuator torques (next)

$$\mathbf{M}(\boldsymbol{\theta})\ddot{\boldsymbol{\theta}} + \mathbf{C}(\boldsymbol{\theta}, \dot{\boldsymbol{\theta}})\dot{\boldsymbol{\theta}} + \boxed{k\boldsymbol{\theta}} + \boxed{\sigma\dot{\boldsymbol{\theta}}} = \boxed{\mathbf{f}(\mathbf{T})}$$

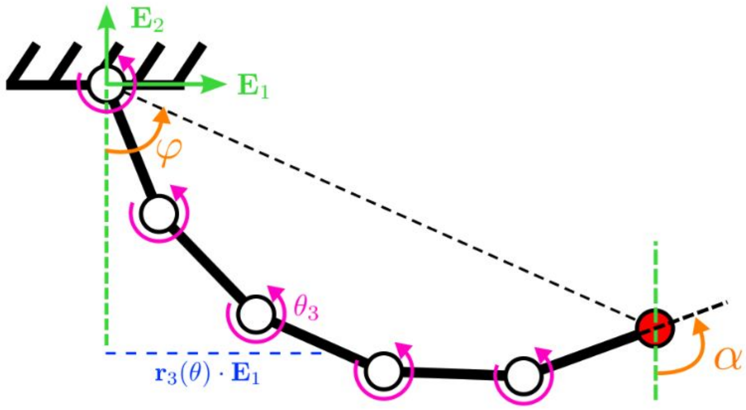

Shape memory alloys (SMA)

- Crystal lattice deformations translate to macroscopic strain

Wikipedia contributors. "Shape-memory alloy." *Wikipedia, The Free Encyclopedia*. Wikipedia, The Free Encyclopedia, 7 Apr. 2022. Web. 25 Apr. 2022.

Shape memory alloys (SMA)

- Crystal lattice deformations translate to macroscopic strain
  - Shape memory effect

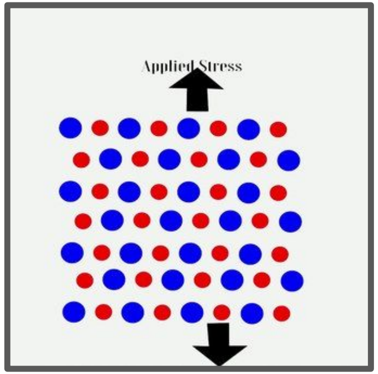

Wikipedia contributors. "Shape-memory alloy." *Wikipedia, The Free Encyclopedia*. Wikipedia, The Free Encyclopedia, 7 Apr. 2022. Web. 25 Apr. 2022.

Single actuation path

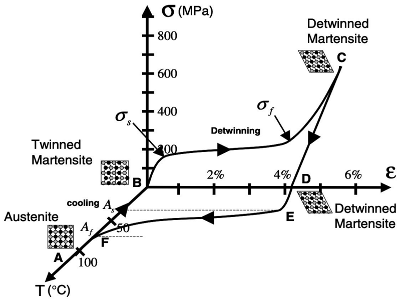

Fig. 1.10. Stress-strain-temperature data exhibiting the shape memory effect for a typical NiTi SMA.

Lagoudas, Dimitris C., ed. *Shape memory alloys: modeling and engineering applications*. Springer Science & Business Media, 2008.

Shape memory alloys (SMA)

- Crystal lattice deformations translate to macroscopic strain
  - Shape memory effect
  - Pseudoelasticity

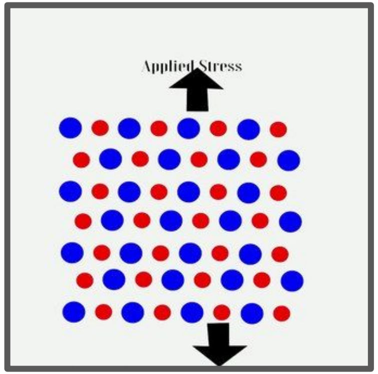

Wikipedia contributors. "Shape-memory alloy." *Wikipedia, The Free Encyclopedia*. Wikipedia, The Free Encyclopedia, 7 Apr. 2022. Web. 25 Apr. 2022.

Lagoudas, Dimitris C., ed. *Shape memory alloys: modeling and engineering applications*. Springer Science & Business Media, 2008.

Single actuation path

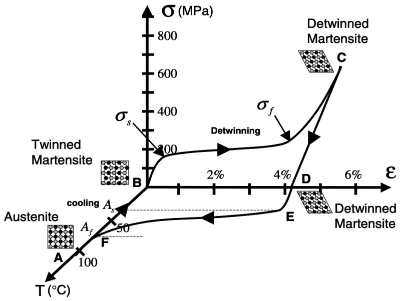

Fig. 1.10. Stress-strain-temperature data exhibiting the shape memory effect for a typical NiTi SMA.

Psuedoelastic loading path

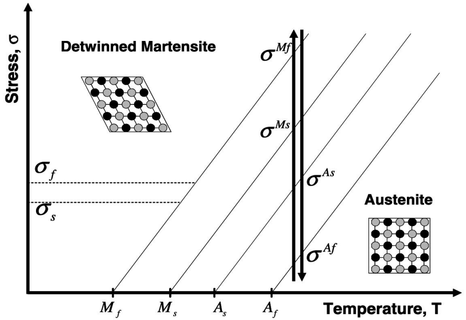

Fig. 1.7. A pseudoelastic loading path.

Shape memory alloys (SMA)

- Crystal lattice deformations translate to macroscopic strain
  - Shape memory effect
  - Pseudoelasticity

Challenges

- Hysteretic effects on stress- and temperature- induced deformations

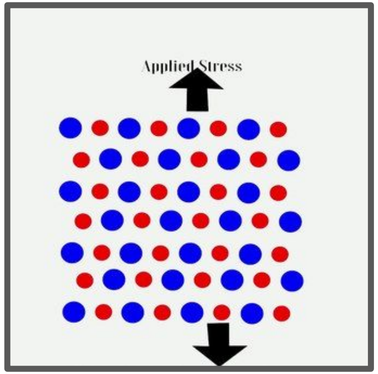

Wikipedia contributors. "Shape-memory alloy." *Wikipedia, The Free Encyclopedia*. Wikipedia, The Free Encyclopedia, 7 Apr. 2022. Web. 25 Apr. 2022.

Lagoudas, Dimitris C., ed. *Shape memory alloys: modeling and engineering applications*. Springer Science & Business Media, 2008.

Single actuation path

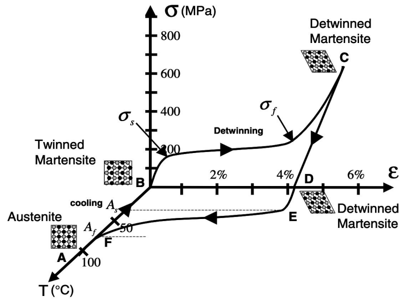

Fig. 1.10. Stress-strain-temperature data exhibiting the shape memory effect for a typical NiTi SMA.

Psuedoelastic loading path

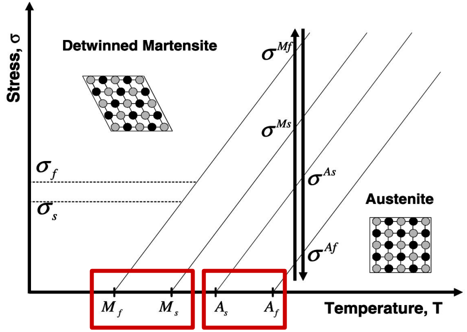

Fig. 1.7. A pseudoelastic loading path.

Shape memory alloys (SMA)

- Crystal lattice deformations translate to macroscopic strain
  - Shape memory effect
  - Pseudoelasticity

Challenges

- Hysteretic effects on stress- and temperature- induced deformations
- Transformation temperatures change based on stress

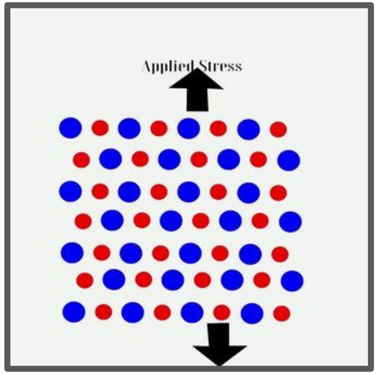

Wikipedia contributors. "Shape-memory alloy." *Wikipedia, The Free Encyclopedia*. Wikipedia, The Free Encyclopedia, 7 Apr. 2022. Web. 25 Apr. 2022.

Lagoudas, Dimitris C., ed. *Shape memory alloys: modeling and engineering applications*. Springer Science & Business Media, 2008.

Single actuation path

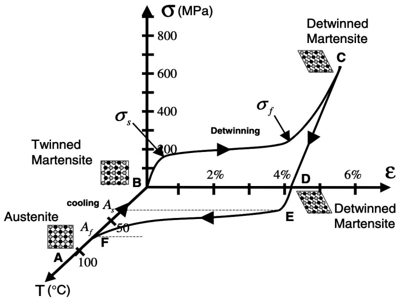

Fig. 1.10. Stress-strain-temperature data exhibiting the shape memory effect for a typical NiTi SMA.

Psuedoelastic loading path

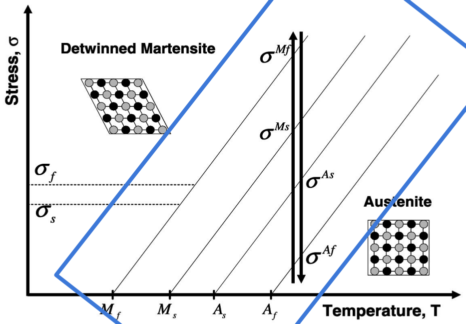

Fig. 1.7. A pseudoelastic loading path.

Shape memory alloys (SMA)

- Crystal lattice deformations translate to macroscopic strain
  - Shape memory effect
  - Pseudoelasticity

Challenges

- Hysteretic effects on stress- and temperature- induced deformations
- Transformation temperatures change based on stress
- Martensite fractions difficult to measure

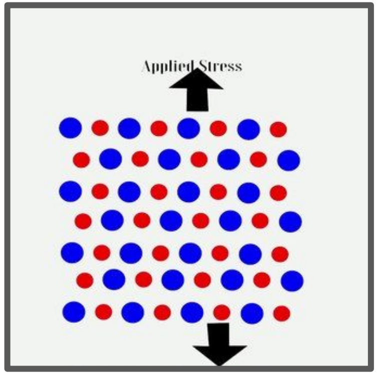

Wikipedia contributors. "Shape-memory alloy." *Wikipedia, The Free Encyclopedia*. Wikipedia, The Free Encyclopedia, 7 Apr. 2022. Web. 25 Apr. 2022.

Lagoudas, Dimitris C., ed. *Shape memory alloys: modeling and engineering applications*. Springer Science & Business Media, 2008.

Single actuation path

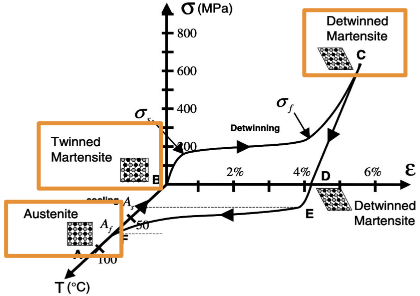

Fig. 1.10. Stress-strain-temperature data exhibiting the shape memory effect for a typical NiTi SMA.

Pseudoelastic loading path

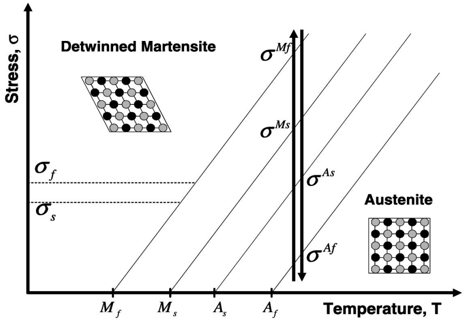

Fig. 1.7. A pseudoelastic loading path.

SMA actuation model

SMA actuation model

Ignore hysteresis

SMA actuation model

Ignore hysteresis

Convective heat transfer model: (ignoring effect of martensite fraction)

Convective cooling   Joule heating

$$\dot{T} = \boxed{a_1(T - T_0)} + \boxed{a_2 D}$$

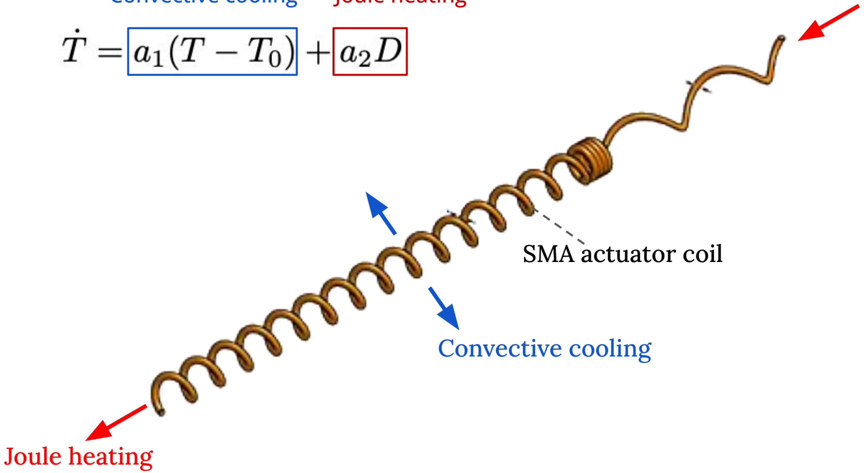

SMA actuation model

Ignore hysteresis

Convective heat transfer model: (ignoring effect of martensite fraction)

Convective cooling Joule heating

$$\dot{T} = \boxed{a_1(T - T_0)} + \boxed{a_2 D},$$
$$\dot{V} = \boxed{a_3(V - T)},$$

Thermal mass of epoxy

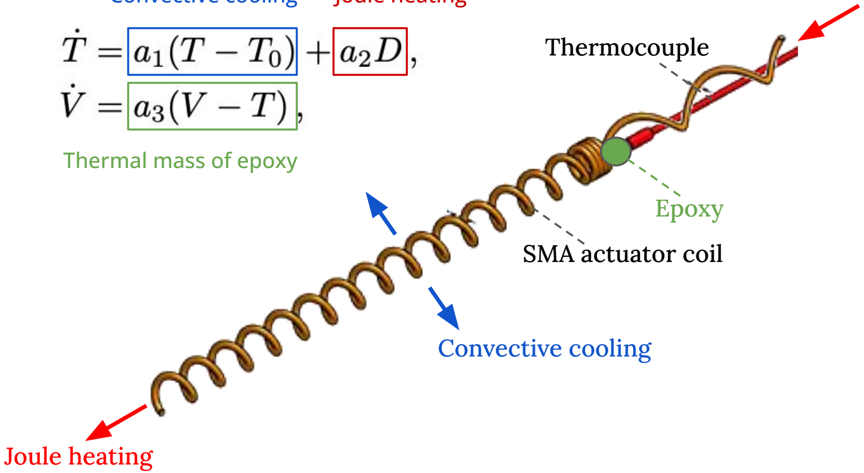

SMA actuation model

Ignore hysteresis

Convective heat transfer model: (ignoring effect of martensite fraction)

Convective cooling | Joule heating

$$\dot{T} = \boxed{a_1(T - T_0)} + \boxed{a_2 D},$$
$$\dot{V} = \boxed{a_3(V - T)},$$

Thermal mass of epoxy

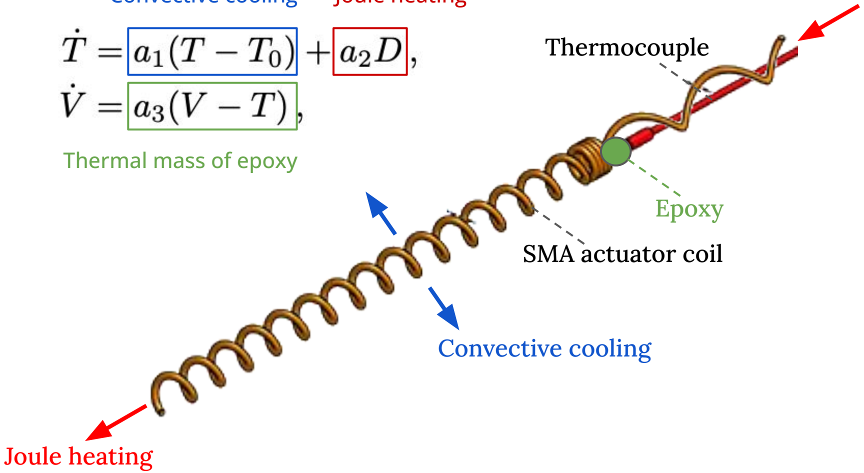

Linear force mapping:

$$\mathbf{f}(\mathbf{T}) = \beta_r(T_r - T_0)\mathbb{1}_{\mathbf{n}} - \beta_l(T_l - T_0)\mathbb{1}_{\mathbf{n}}.$$

SMA actuation model

Ignore hysteresis

Convective heat transfer model: (ignoring effect of martensite fraction)

Convective cooling — Joule heating

$$\dot{T} = \boxed{a_1(T - T_0)} + \boxed{a_2 D},$$
$$\dot{V} = \boxed{a_3(V - T)},$$

Thermal mass of epoxy

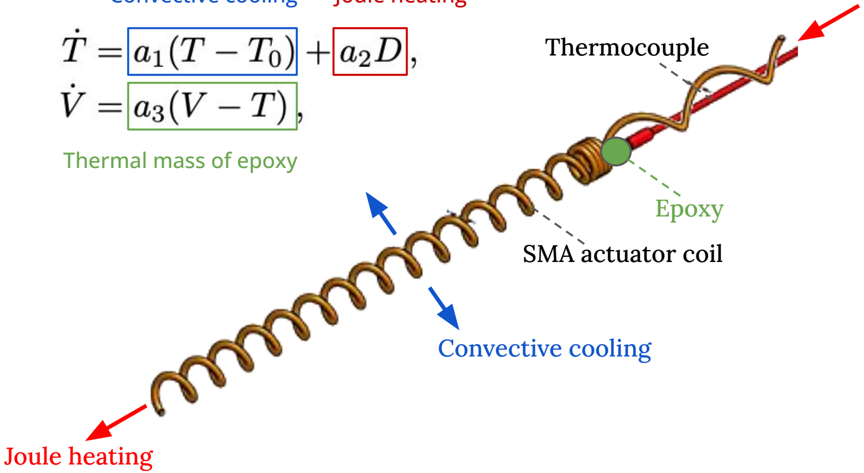

Linear force mapping:

$$\mathbf{f}(\mathbf{T}) = \beta_r(T_r - T_0)\mathbb{1}_{\mathbf{n}} - \beta_l(T_l - T_0)\mathbb{1}_{\mathbf{n}}.$$

- Reasonable for some operating conditions, not all
- Ignores martensite fraction
- Assumes linear relationship between martensite fraction and temperature

Complete dynamics block

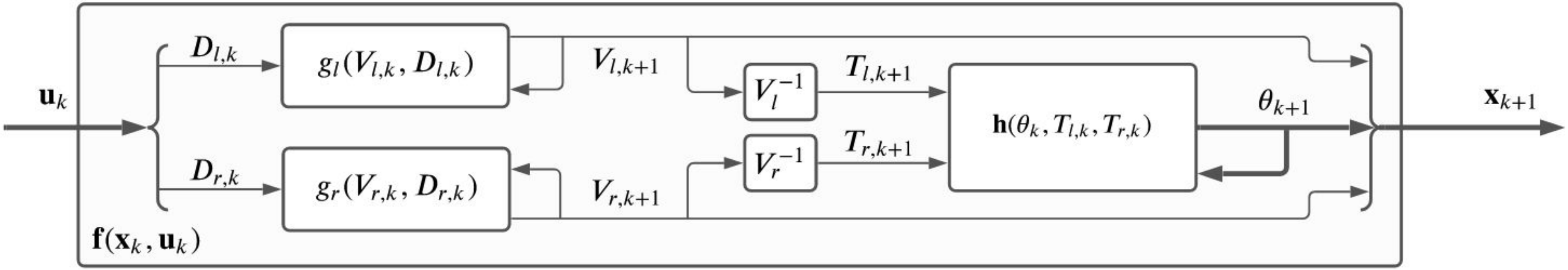

Complete dynamics block

Control inputs

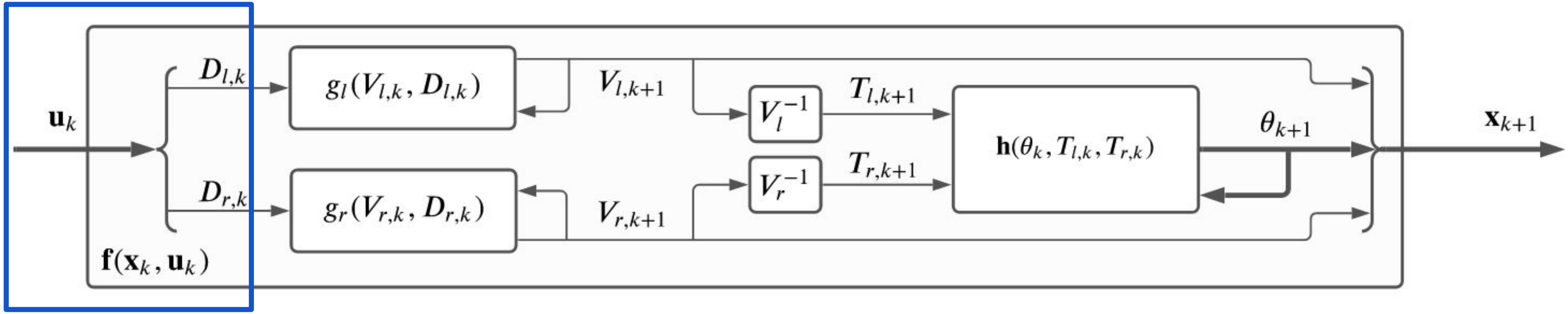

Complete dynamics block

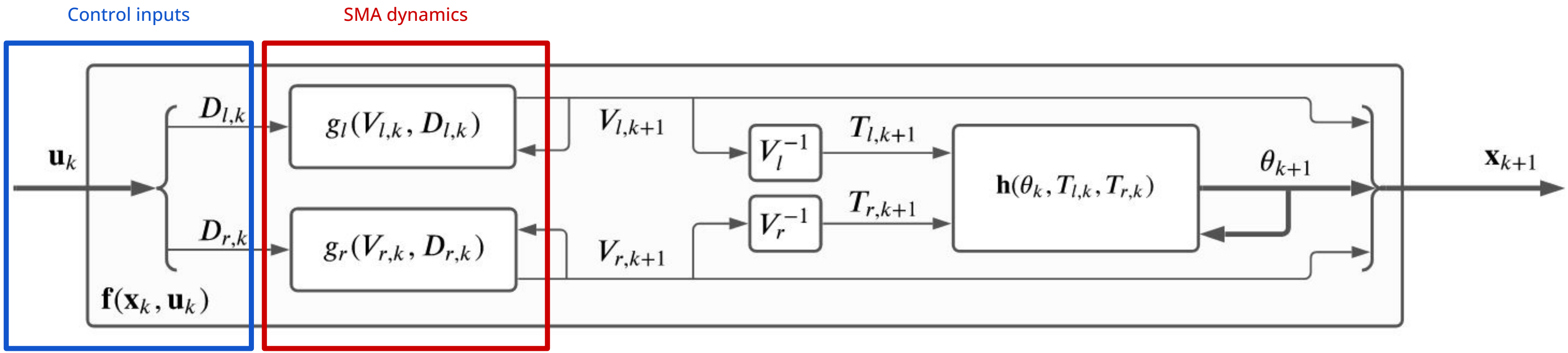

Complete dynamics block

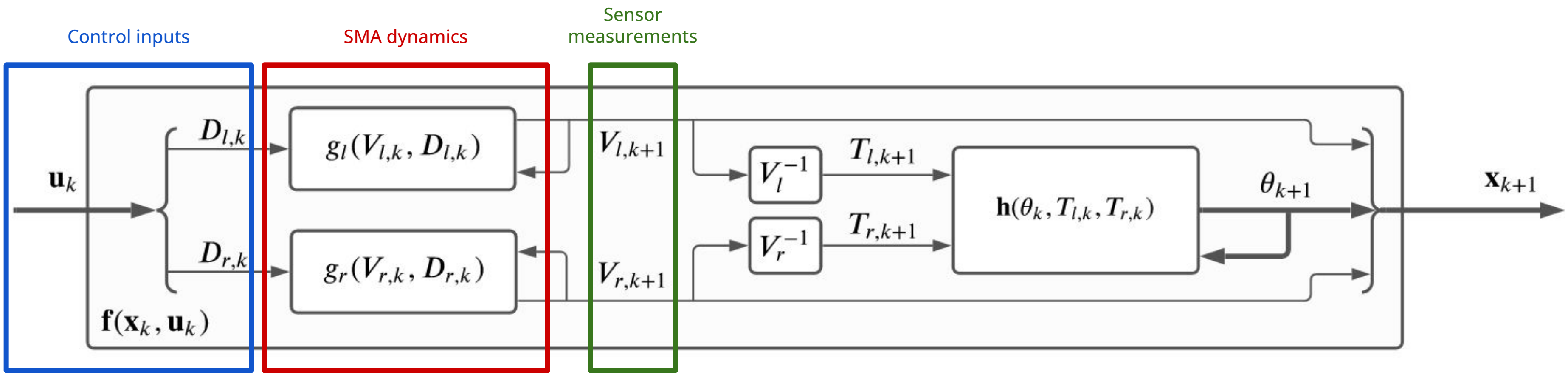

Complete dynamics block

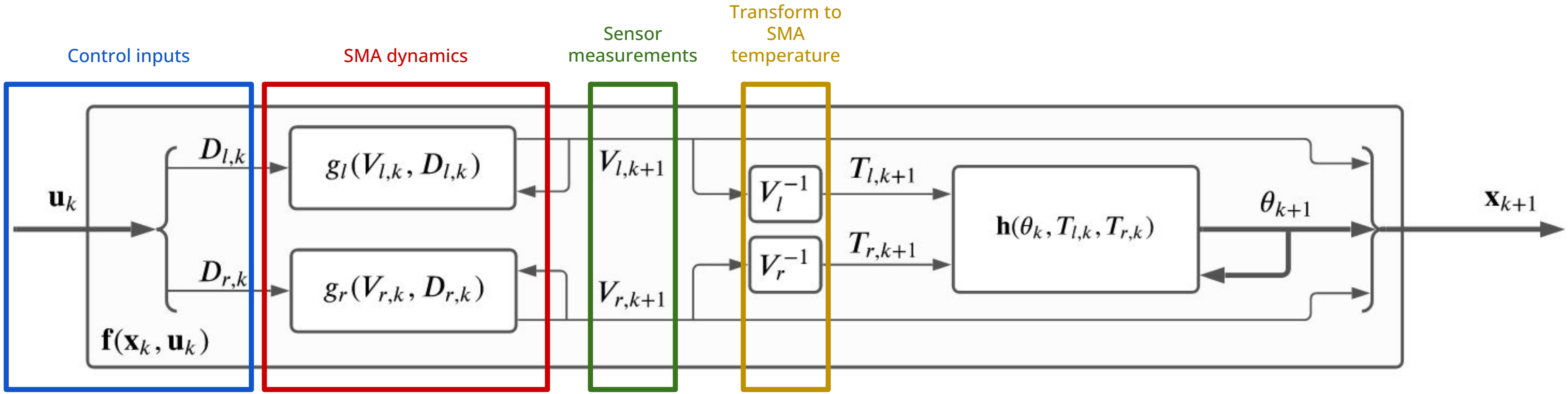

Complete dynamics block

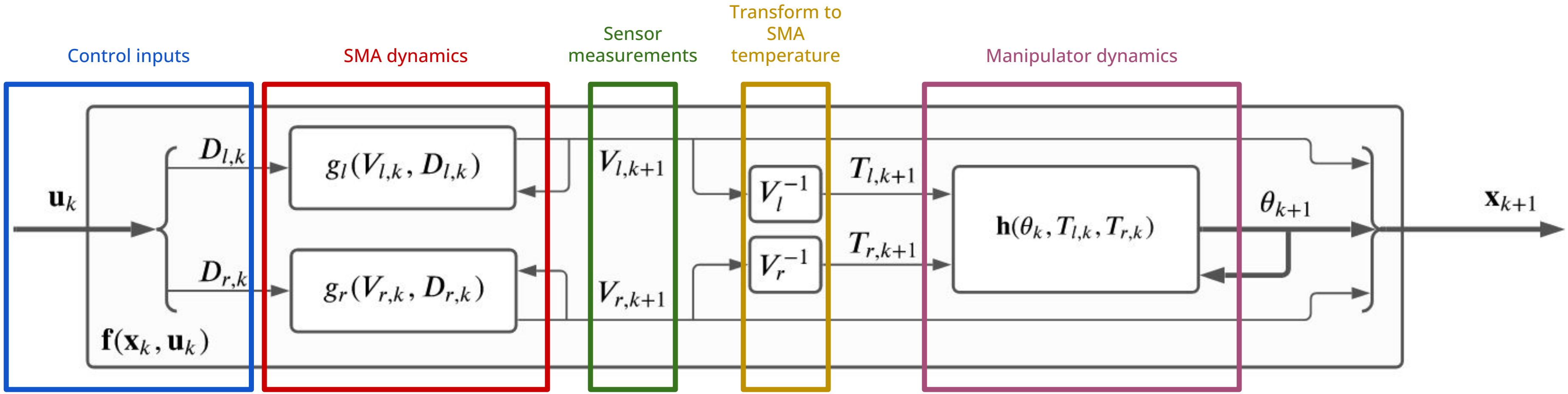

Complete dynamics block

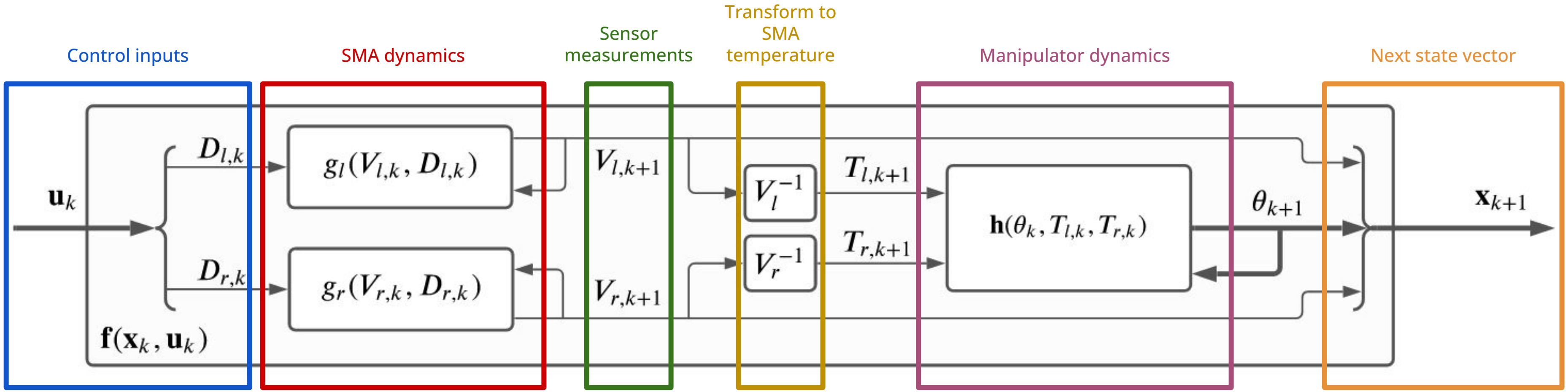

Kinematics Modeling

Constant curvature, Euler-Bernoulli beam

Constant curvature assumption

Assuming uniform actuator torques and

Manipulator joint angle i

$$\theta_i = 2\varphi/(n+1), \qquad \forall i = 1 \ldots n.$$

Bend angle

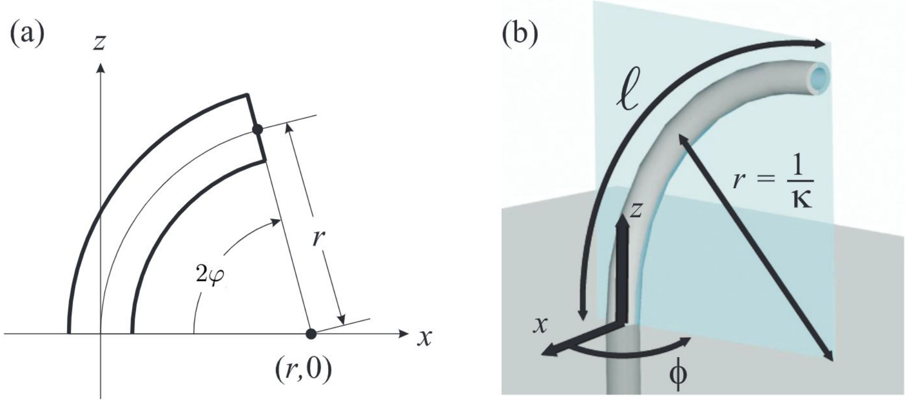

Webster III, Robert J., and Bryan A. Jones. "Design and kinematic modeling of constant curvature continuum robots: A review." *The International Journal of Robotics Research* 29.13 (2010): 1661-1683.
Modified from figure 3.

Euler-Bernoulli beam assumption under gravity

Successive joint angles decrease exponentially.

Manipulator joint angle i at equilibrium

$$\theta_i^{eq} = \lambda \varphi^{eq} \frac{(N-i+1)^2}{\sum_{j=1}^{N}(N-j)^2}$$

Bend angle at equilibrium

Material-dependent scaling parameter

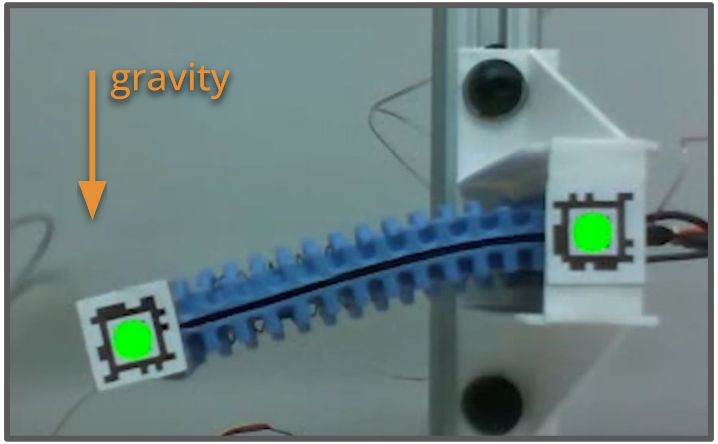

Data Collection & Model Calibration

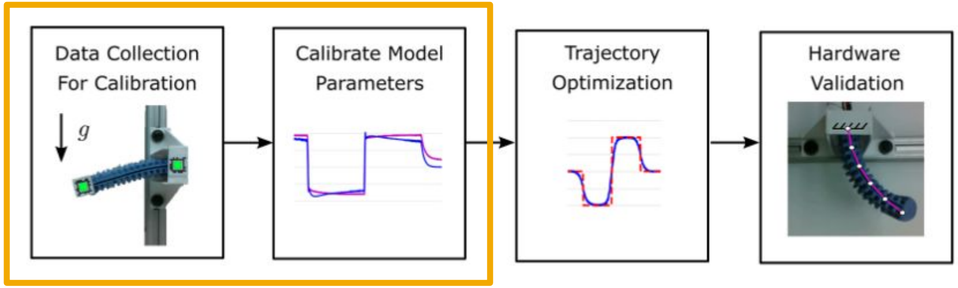

Torsional spring coefficient

- Limb was rotated 90°, left to bend under gravity
- Simplified dynamics:

$$k\boldsymbol{\theta}^{eq} + \mathbf{f_g}(\boldsymbol{\theta}^{eq}) = \mathbf{0}$$

- Bend angle measured at static equilibrium
- Constant curvature does not apply; use EB kinematics

$$\theta_i^{eq} = \lambda\varphi^{eq}\frac{(N-i+1)^2}{\sum_{j=1}^{N}(N-j)^2} = \lambda\varphi^{eq}b_i$$

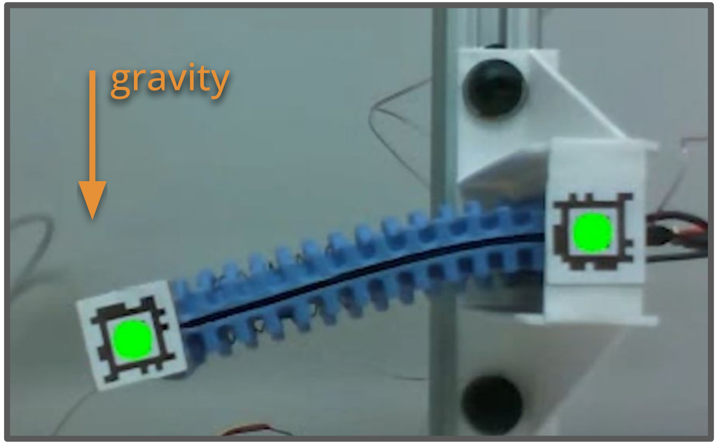

$$U_g(\boldsymbol{\theta}^{eq}) = mg\sum_{i=1}^{n}\mathbf{r_i}(\boldsymbol{\theta}^{eq}) \cdot \mathbf{E_1}$$

$$\mathbf{f_g}(\boldsymbol{\theta}^{eq}) = -\nabla_{\boldsymbol{\theta}}U_g(\boldsymbol{\theta}^{eq})$$

$$k = -\boldsymbol{\theta}^{eq} \setminus \mathbf{f_g}(\boldsymbol{\theta}^{eq})$$

Damping coefficient

- Release limb tip from bent position and collect data from damped oscillation
- Dynamics:

$$\mathbf{M}(\boldsymbol{\theta})\ddot{\boldsymbol{\theta}} + \mathbf{C}(\boldsymbol{\theta}, \dot{\boldsymbol{\theta}})\dot{\boldsymbol{\theta}} + k\boldsymbol{\theta} + \sigma\dot{\boldsymbol{\theta}} = \mathbf{0}\,.$$

- CC does not apply.
- EB difficult to apply without forces.
- Instead, nested optimization:
  - Fit a damped sinusoid to bend angle trajectory
  - Find the damping coefficient which produces the closest fit

Algorithm 1: Nested optimization to find σ by matching the damping observed in hardware data $\varphi^d_{1\ldots t}$.

Procedure `fitDS` $(\varphi_{1\ldots t}) \rightarrow \sigma^*$:

$\zeta^*, \omega_n^* \leftarrow \arg\min ||\varphi_{1\ldots t} - Ae^{-\zeta\omega_n t}\sin(\omega_n\sqrt{1-\zeta^2}t + \phi) + b||_2^2$

$\sigma^* \leftarrow \zeta^*\omega_n^*$

Procedure `fitData` $(\varphi^d_{1\ldots t}) \rightarrow \sigma^*_{mdl}$:

$\sigma_d^* \leftarrow \texttt{fitDS}(\varphi^d_{1\ldots t})$

$\sigma^*_{mdl} \leftarrow \arg\min ||\sigma_d^* - \texttt{fitDS}(\varphi^{mdl}_{1\ldots t}|\sigma_{mdl})||_2^2$

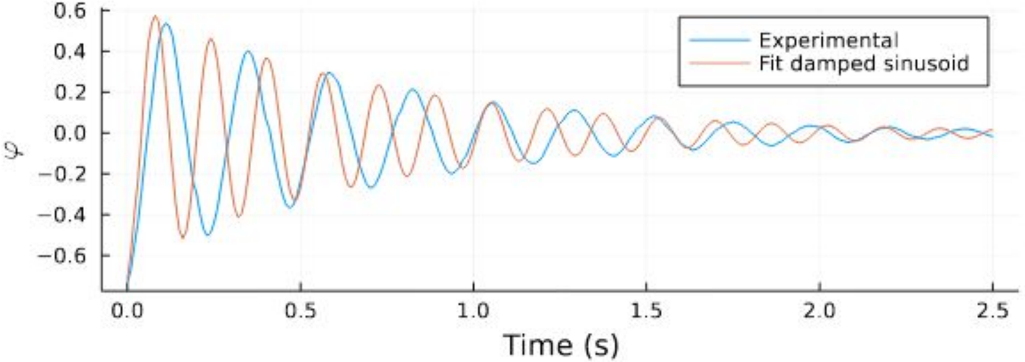

Thermal actuator calibration setup

- Collect data under three conditions:

$$\mathbf{f}(\mathbf{T}^{eq}) \neq \mathbf{0}, \dot{\varphi} = 0, \dot{\mathbf{V}} = \mathbf{0}$$

1. Actuated,
2. Static equilibrium,
3. Thermal equilibrium.

- Then make three assumptions:

1. $\mathbf{V}^{eq} = \mathbf{T}^{eq}$
2. $k\boldsymbol{\theta}^{eq} = \frac{2k\varphi^{eq}}{(n+1)} \mathbb{1}_{\mathbf{n}} = [\beta_r(T_r^{eq} - T_0) - \beta_l(T_l^{eq} - T_0)]\, \mathbb{1}_{\mathbf{n}}$
3. $\mathbf{V}^{eq} \neq 0 \Rightarrow \varphi^{eq} \neq 0$

Thermal actuator heat transfer coefficients

- Collect data under three conditions:

$$\mathbf{f}(\mathbf{T}^{eq}) \neq \mathbf{0}, \dot{\varphi} = 0, \dot{\mathbf{V}} = \mathbf{0}$$

1. Actuated,
2. Static equilibrium,
3. Thermal equilibrium.

- Then make three assumptions:
  1. $\mathbf{V}^{eq} = \mathbf{T}^{eq}$
  2. $k\boldsymbol{\theta}^{eq} = \frac{2k\varphi^{eq}}{(n+1)} \mathbb{1}_{\mathbf{n}} = [\beta_r(T_r^{eq} - T_0) - \beta_l(T_l^{eq} - T_0)]\,\mathbb{1}_{\mathbf{n}}$
  3. $\mathbf{V}^{eq} \neq 0 \Rightarrow \varphi^{eq} \neq 0.$

- From assumptions 1 & 2,

$$T_j^{eq} = b\varphi^{eq} + T_0, \quad b = \frac{V^{eq} - T_0}{\varphi^{eq}}$$

- Use relationship to roughly scale the rest of the time series:

$$T_{j,1\ldots t} = b\varphi_{1\ldots t} + T_0$$

- With T, V, and D known, fit system of ODEs using Julia DiffEqParamEstim.jl package

$$\dot{T} = a_1(T - T_0) + a_2 D\,,$$
$$\dot{V} = a_3(V - T)\,,$$

Thermal actuator force coefficients

- Collect data under three conditions:

$$\mathbf{f}(\mathbf{T}^{eq}) \neq \mathbf{0}, \dot{\varphi} = 0, \dot{\mathbf{V}} = \mathbf{0}$$

1. Actuated,
2. Static equilibrium,
3. Thermal equilibrium.

- Then make three assumptions:
  1. $\mathbf{V}^{eq} = \mathbf{T}^{eq}$
  2. $k\boldsymbol{\theta}^{eq} = \frac{2k\varphi^{eq}}{(n+1)} \mathbb{1}_{\mathbf{n}} = [\beta_r(T_r^{eq} - T_0) - \beta_l(T_l^{eq} - T_0)]\, \mathbb{1}_{\mathbf{n}}$
  3. $\mathbf{V}^{eq} \neq 0 \Rightarrow \varphi^{eq} \neq 0.$

- From assumption 2, observe

$$\beta_j = [k/(T_j^{eq} - T_0)]\theta_i^{eq}.$$

- Take all such points, stack in vector:

$$\boldsymbol{\Gamma}_j^{eq} = \begin{bmatrix} (k/(T_{j1}^{eq} - T_0))\, \theta_{i1}^{eq} \\ \vdots \\ (k/(T_{jt}^{eq} - T_0))\, \theta_{it}^{eq} \end{bmatrix}$$

- Then compute directly:

$$\beta_j = \mathbb{1}_{\mathbf{t}} \backslash \boldsymbol{\Gamma}_j^{eq}$$

Good model calibration agreement

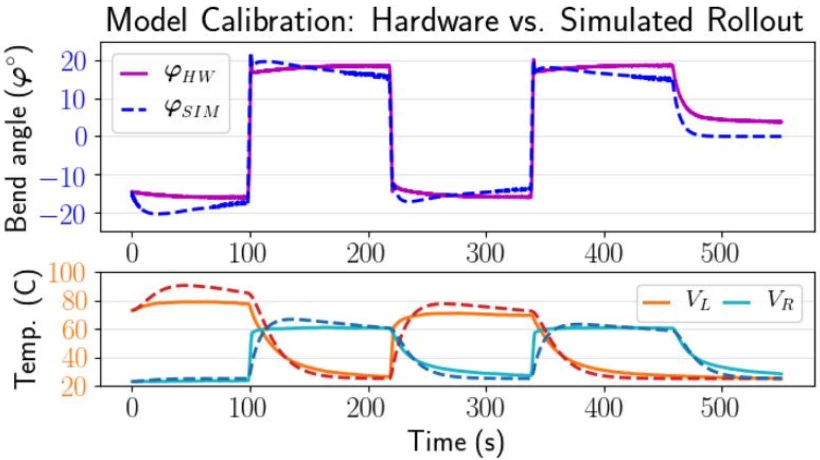

Trajectory optimization

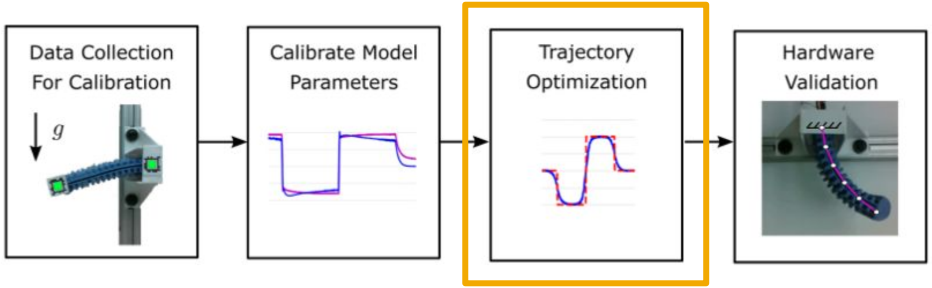

Optimization setup

Quadratic-cost optimization

- Q (tracking error penalties) only cares about positions
- R (control penalties) included to minimize control signals

Constraints:

1. Initial condition
2. System dynamics
3. Valid controls
4. Safe temperatures
5. Warm operation

Optimized feasible state trajectory — Optimized open-loop control trajectory — Tracking error

$$\mathbf{x}^*_{1\ldots N}, \mathbf{u}^*_{1\ldots N} = \arg\min_{\mathbf{x},\mathbf{u}} \frac{1}{2}\sum_{k=1}^{N-1}\left(\tilde{\mathbf{x}}_\mathbf{k}{}^\top \mathbf{Q}\tilde{\mathbf{x}}_\mathbf{k} + \mathbf{u}_\mathbf{k}{}^\top \mathbf{R}\mathbf{u}_\mathbf{k}\right) + \frac{1}{2}\tilde{\mathbf{x}}_\mathbf{N}{}^\top \mathbf{Q}_\mathbf{N}\tilde{\mathbf{x}}_\mathbf{N}$$

$$\begin{aligned}
\text{s.t.}\quad & \mathbf{x_1} = \mathbf{x}_{\text{init}} \\
& \mathbf{x_{k+1}} = \mathbf{f}(\mathbf{x_k}, \mathbf{u_k}) \\
& \mathbf{0} \leq \mathbf{u_k} \leq \mathbb{1}_\mathbf{2} \\
& \mathbf{T_k} < T_{max}\mathbb{1}_\mathbf{2} \\
& \mathbf{T_k} > T_{warm}\mathbb{1}_\mathbf{2} \qquad \forall k > k_{warm}\,.
\end{aligned}$$

Optimization results

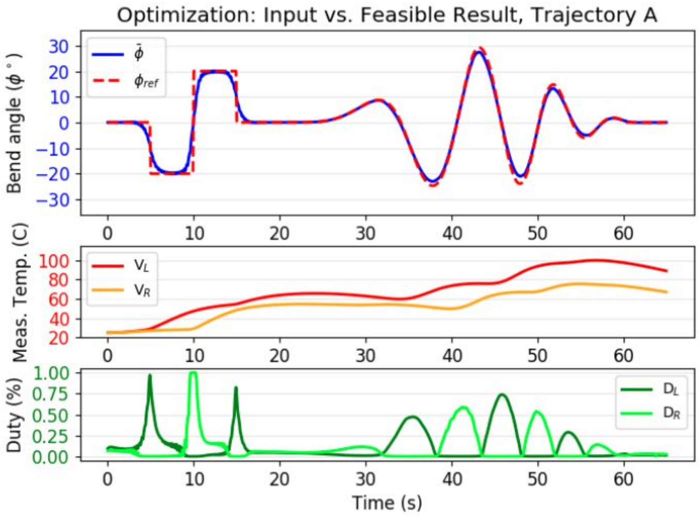

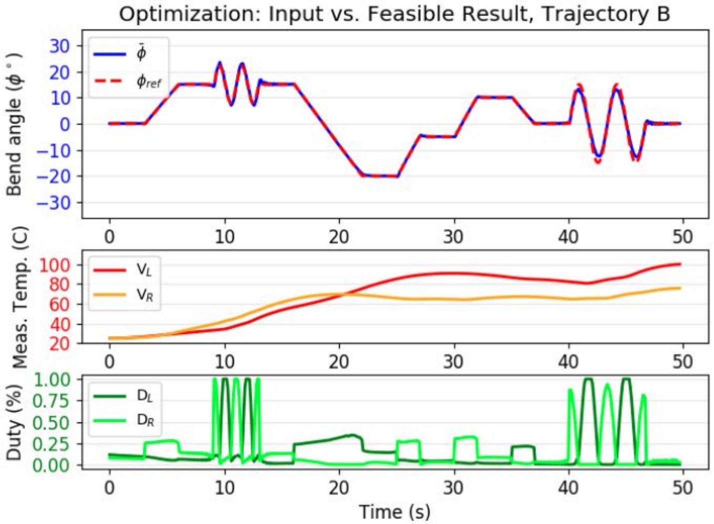

Open-loop Tracking Results

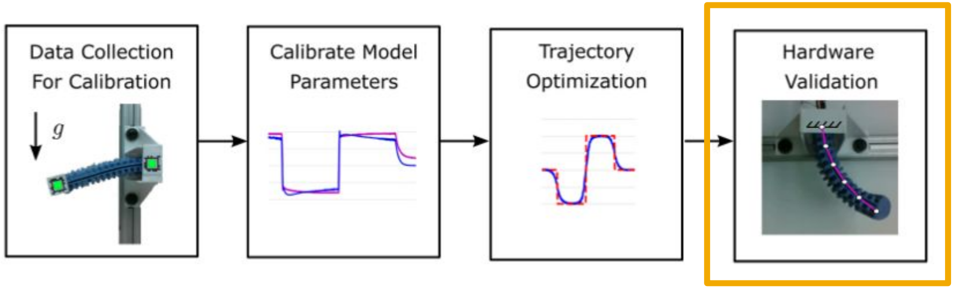

Hardware validation

- Hardware tracking good, but improvement is needed

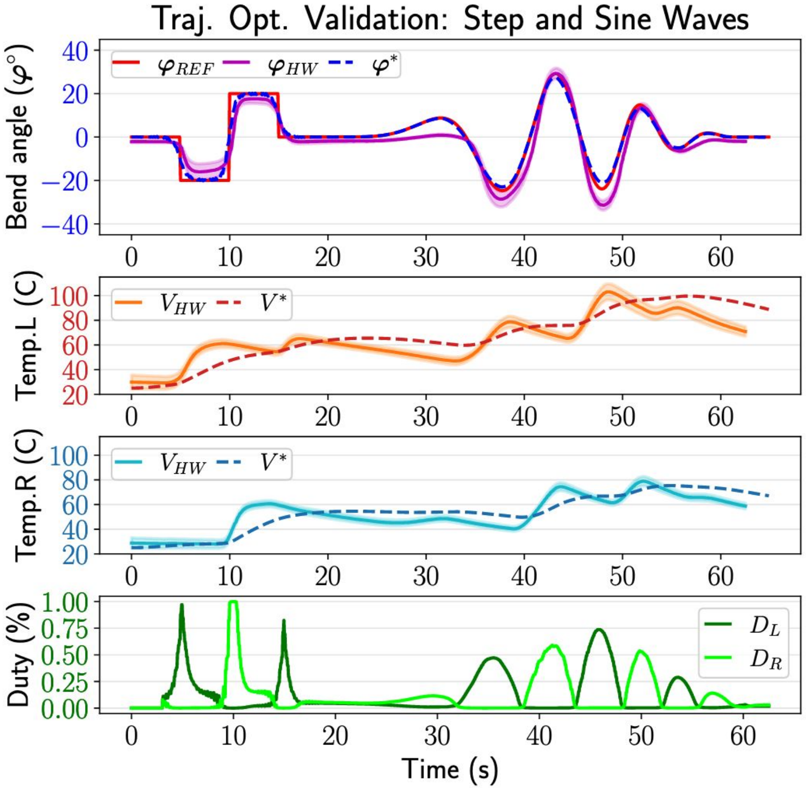

Hardware validation

- Hardware tracking good, but improvement is needed
- "Soft" startups difficult

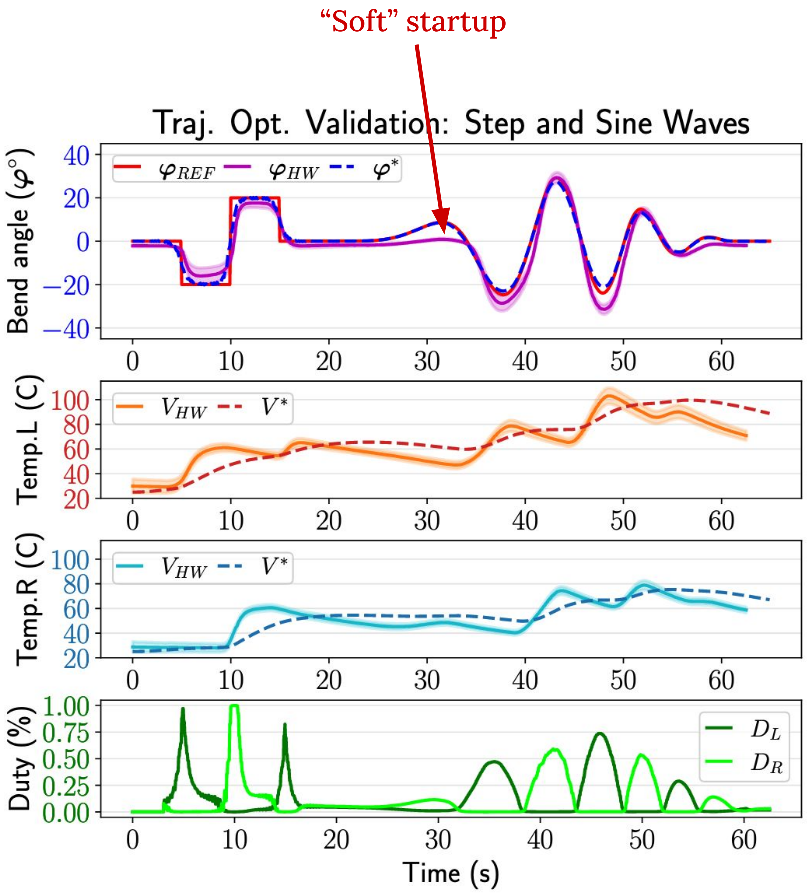

Hardware validation

- Hardware tracking good, but improvement is needed
- “Soft” startups difficult
- Some tracking bias observed

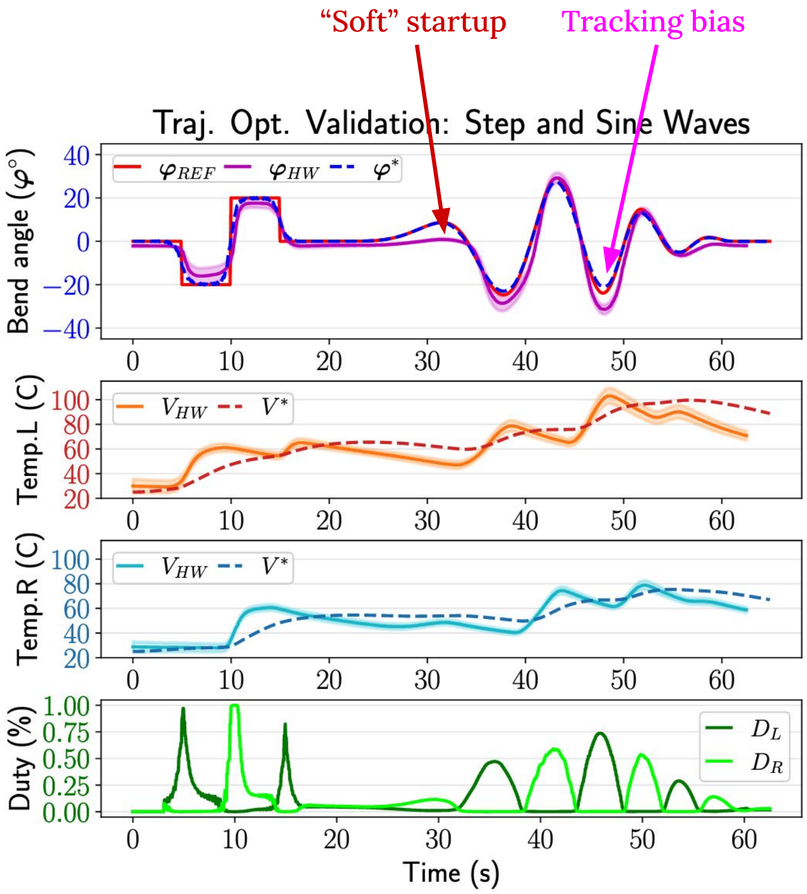

Hardware validation

- Hardware tracking good, but improvement is needed
- "Soft" startups difficult
- Some tracking bias observed
- Temperature does not track well

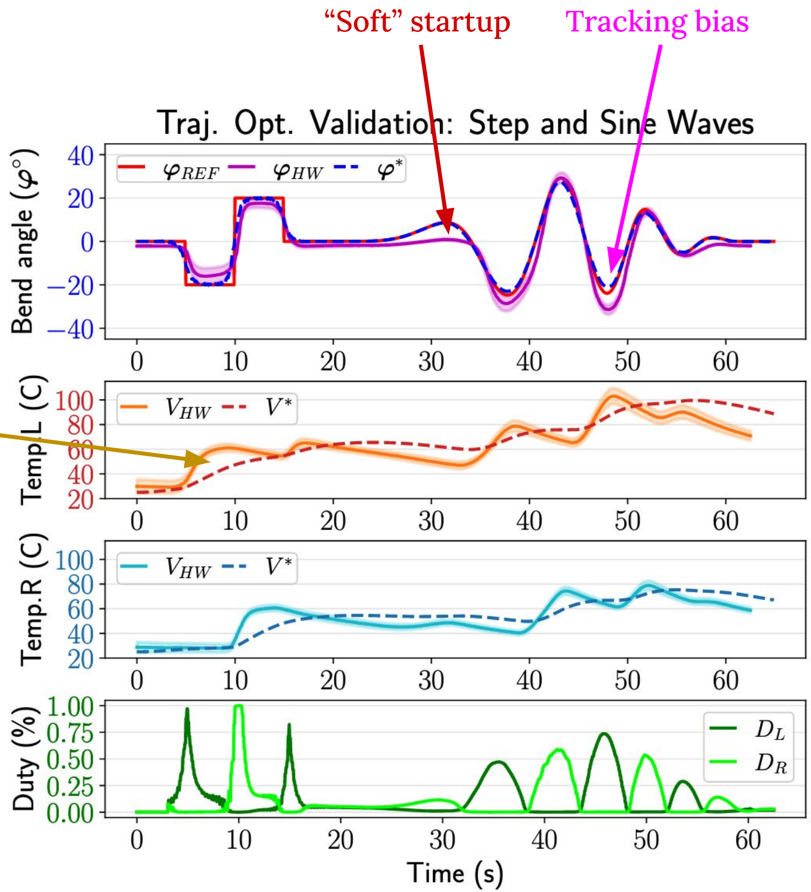

Hardware validation

- Hardware tracking good, but improvement is needed
- "Soft" startups difficult
- Some tracking bias observed
- Temperature does not track well
  - Timescale of original validation too long

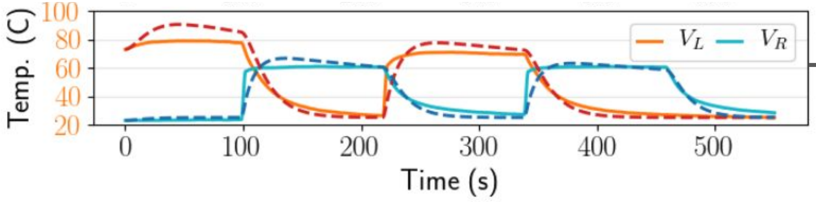

  - Thermal model fit motion dynamics well ("T") but not observations ("V")

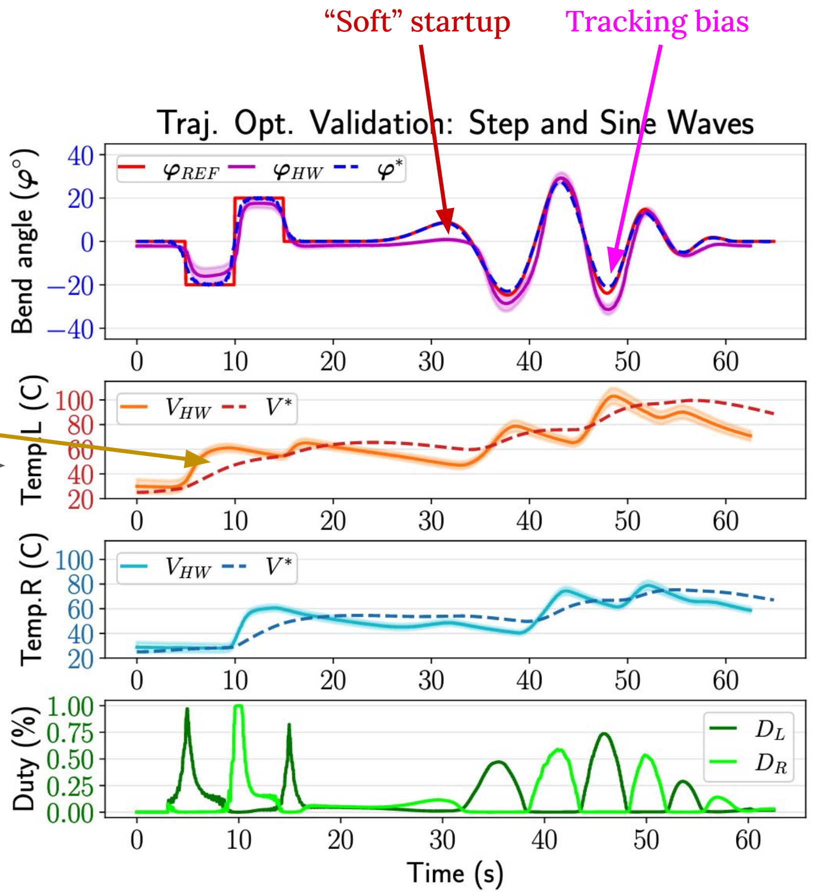

Teach -and- Repeat

Teach-and-repeat results

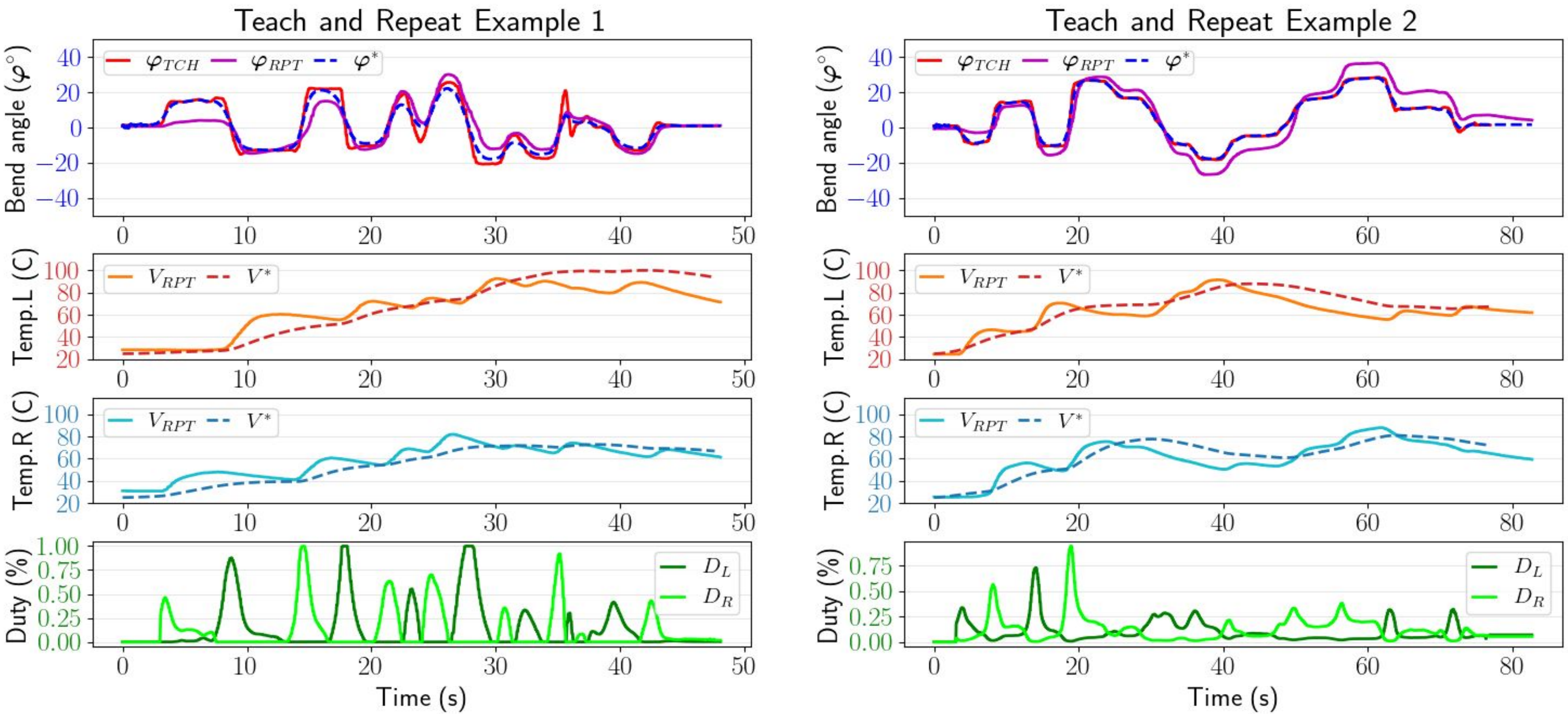

Future Work

Future Work

- Improvements to SMA force model
  - At least rudimentary modeling of hysteresis

Shape memory alloy hysteresis [1]

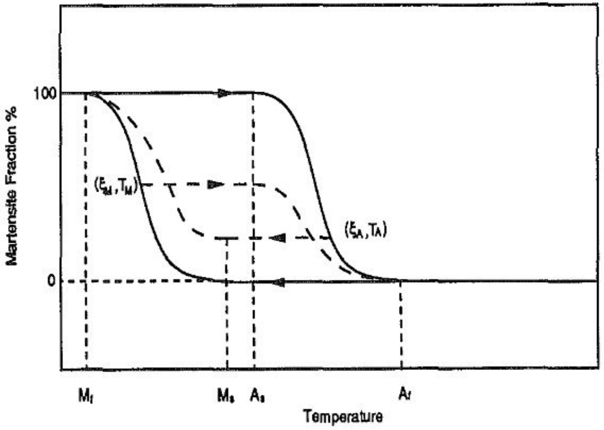

[1] Liang, Chen, and Craig A. Rogers. "One-dimensional thermomechanical constitutive relations for shape memory materials." *Journal of intelligent material systems and structures* 8.4 (1997): 285-302.

Future Work

- Improvements to SMA force model
  - At least rudimentary modeling of hysteresis
  - Better stress mapping, especially outside linear region

Shape memory alloy hysteresis [1]

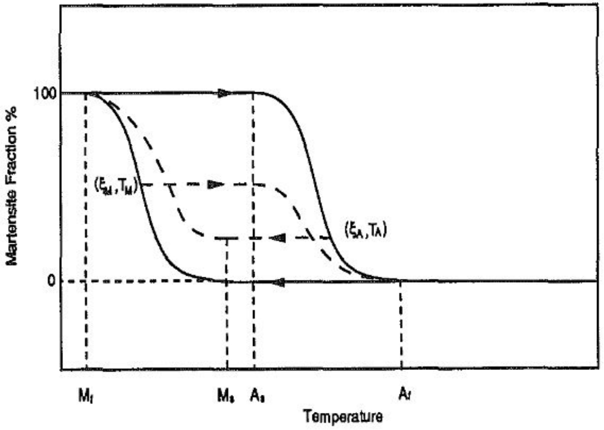

SMA unified constitutive relation [2]

$$\tau - \tau_0 = G(\xi)(\gamma - \gamma_0) + \frac{\Theta}{\sqrt{3}}(T - T_0) + \frac{\Omega(\xi)}{\sqrt{3}}(\xi - \xi_0)$$

[1] Liang, Chen, and Craig A. Rogers. "One-dimensional thermomechanical constitutive relations for shape memory materials." *Journal of intelligent material systems and structures* 8.4 (1997): 285-302.

[2] Cheng, Shing Shin, Yeongjin Kim, and Jaydev P. Desai. "Modeling and characterization of shape memory alloy springs with water cooling strategy in a neurosurgical robot." *Journal of intelligent material systems and structures* 28.16 (2017): 2167-2183.

Future Work

- Improvements to SMA force model
  - At least rudimentary modeling of hysteresis
  - Better stress mapping, especially outside linear region
- Improvements to SMA temperature model
  - Higher priority on matching measurement temperature

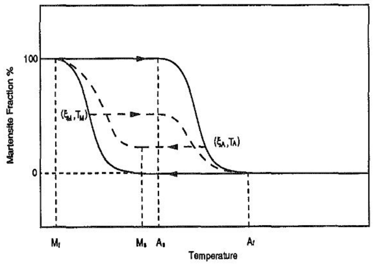

$$\tau - \tau_0 = G(\xi)(\gamma - \gamma_0) + \frac{\Theta}{\sqrt{3}}(T - T_0) + \frac{\Omega(\xi)}{\sqrt{3}}(\xi - \xi_0)$$

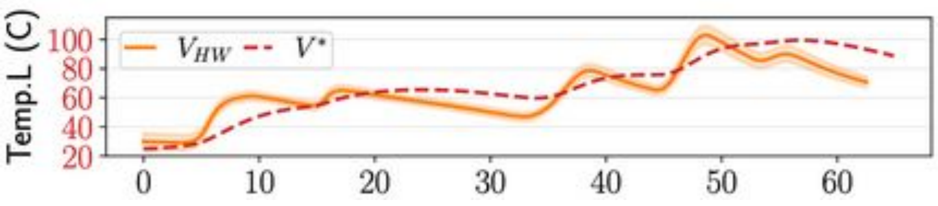

Future Work

- Improvements to SMA force model
  - At least rudimentary modeling of hysteresis
  - Better stress mapping, especially outside linear region
- Improvements to SMA temperature model
  - Higher priority on matching measurement temperature
- Investigate use of ML models to model residual error

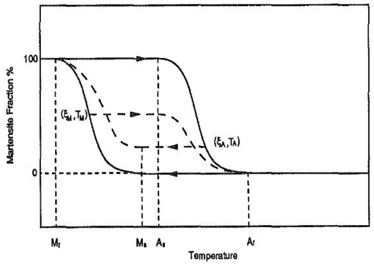

$$\tau - \tau_0 = G(\xi)(\gamma - \gamma_0) + \frac{\Theta}{\sqrt{3}}(T - T_0) + \frac{\Omega(\xi)}{\sqrt{3}}(\xi - \xi_0)$$

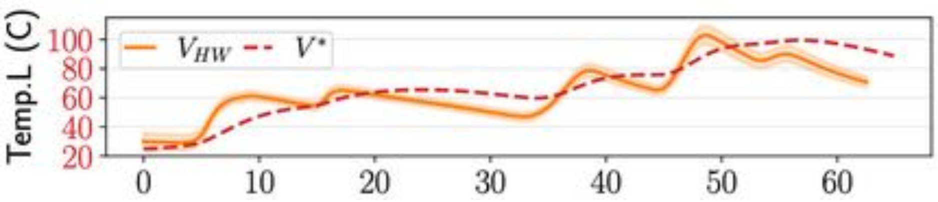

Future Work

- Improvements to SMA force model
  - At least rudimentary modeling of hysteresis
  - Better stress mapping, especially outside linear region
- Improvements to SMA temperature model
  - Higher priority on matching measurement temperature
- Investigate use of ML models to model residual error and bias
- Extend to multi-link system
  - Full Horton robot is composed of five links (three legs, two shoulders)

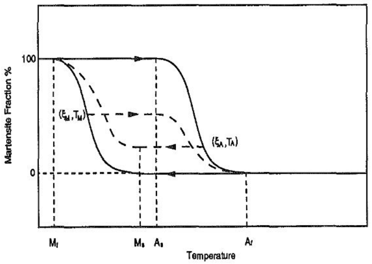

$$\tau - \tau_0 = G(\xi)(\gamma - \gamma_0) + \frac{\Theta}{\sqrt{3}}(T - T_0) + \frac{\Omega(\xi)}{\sqrt{3}}(\xi - \xi_0)$$

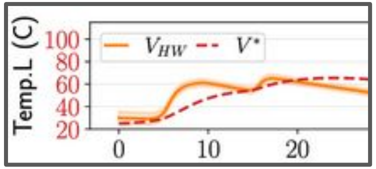

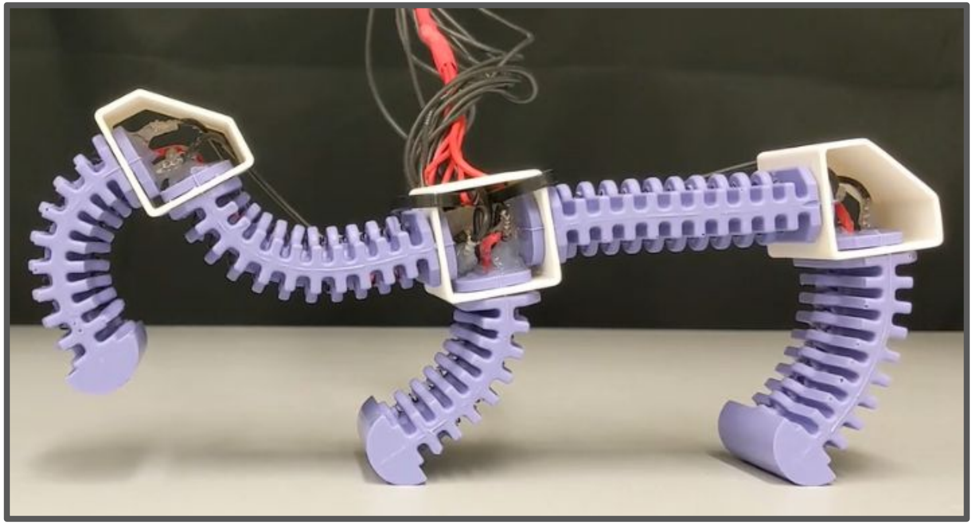

Final remarks

Main contributions		

Final remarks

Main contributions		
Development and calibration of simplified models for thermal-actuation and soft manipulator dynamics.		
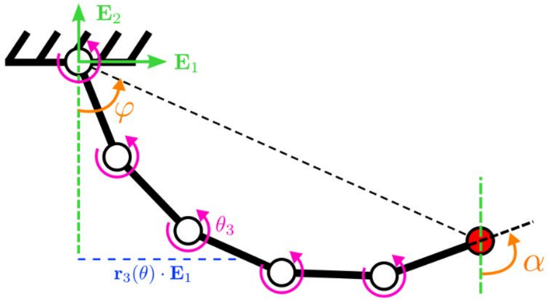		

Final remarks

Main contributions		
Development and calibration of simplified models for thermal-actuation and soft manipulator dynamics.	Design of feasible trajectories and open-loop controls through optimization.	
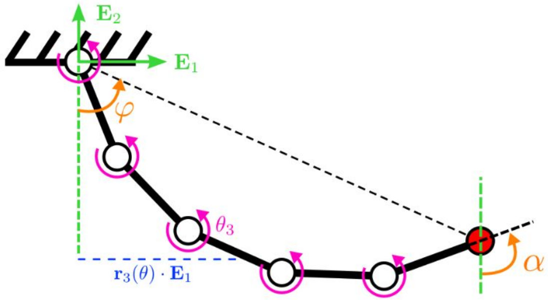	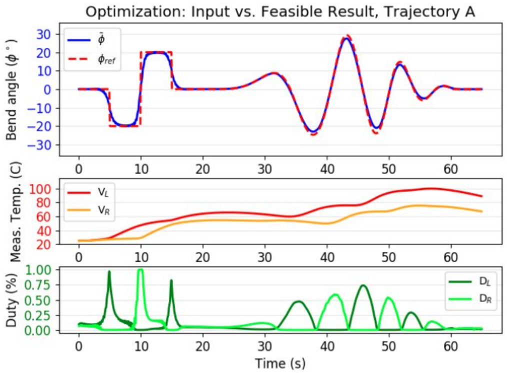	

Final remarks

Main contributions		
Development and calibration of simplified models for thermal-actuation and soft manipulator dynamics.	Design of feasible trajectories and open-loop controls through optimization.	Validation in hardware using an SMA-actuated soft manipulator.